

Charmonium radiative transitions, meson and glueball particle properties with the effective strong coupling

Gurjav Ganbold^{1,2,*}

¹Bogoliubov Laboratory of Theoretical Physics, JINR, Dubna 141980, Russia

²Institute of Physics and Technology, Ulaanbaatar 13330, Mongolia

Abstract. The particle properties of conventional mesons and scalar glueball, radiative transitions of charmonium excited states χ_{cJ} ($J = 0, 1, 2$) are studied in the framework of relativistic quark models with infrared confinement by taking into account the mass dependence of the effective strong coupling. A specific behaviour of the mass-dependent strong coupling with a freezing point $\alpha_s(0) = 1.032$ has been revealed. The spectrum and leptonic (weak) decay constants of conventional mesons have been calculated in good agreement with the latest experimental data. New estimates on the scalar glueball mass, 'radius' and gluon condensate value have been obtained. Dominant radiative transitions of the charmonium orbital excitations $\chi_{cJ} \rightarrow J/\Psi + \gamma$ have been studied and the partial decay widths have been estimated with reasonable accuracy.

1 Introduction

In modern particle physics one deals with a number of phenomena such as the quark confinement, running strong coupling, generation of hadron mass etc., which require correct description of hadron dynamics in the low-energy domain within theoretical models. QCD predicts a dependence of the physical strong coupling under changes of energy (or, mass) scale Q . This dependence $\alpha_s(Q) \doteq g^2/(4\pi)$ is determined well in experiments at relatively high energies [1]. Meanwhile, the low-energy (or, infrared - IR) behavior of α_s has not been well defined yet, it needs to be more specified, because many quantities in particle physics are affected by the IR behavior of α_s . The correct description of QCD effective coupling in the IR regime remains one of the important problems. The hadron mass origin is one of the challenges to particle physics because the Standard Model introduces only fundamental particles and does not explain the appearance of the multitude of observed massive hadrons. The calculation of hadron mass spectra qualitatively comparable to the precise experimental data, still remains a key problem. Recently, the Particle Data Group [2] has reported that the treatment of the branching ratios of the charmonium excited states χ_{cJ} ($J = 0, 1, 2$) have undergone an important restructuring. The study of the properties of χ_{cJ} mesons is of great interest due to some of their outstanding features.

Our study is based on the formalism of analytic (infrared) confinement principle [3] and the Covariant Confined Quark Model (CCQM) [4].

*e-mail: ganbold@theor.jinr.ru

2 Model with infrared confinement

One of the theoretical approaches explaining the non-observation of quarks is the Analytic Confinement model assuming entire analytic *nonlocal* functions for the quark and gluon propagators [3]. The QCD-inspired model Lagrangian reads [5]:

$$\mathcal{L} = -\frac{1}{4} \left(\partial^\mu \mathcal{A}_\nu^A - \partial^\nu \mathcal{A}_\mu^A + g f^{ABC} \mathcal{A}_\mu^B \mathcal{A}_\nu^C \right)^2 + \left(\bar{q}_f^a \left[\gamma_\alpha \partial^\alpha - m_f \right] q_f^b \right) + g \left(\bar{q}_f^a \left[\Gamma_C^\alpha \mathcal{A}_\alpha^C \right] q_f^b \right), \quad (1)$$

where \mathcal{A}_α^C is the gluon and q_f^a is a quark field of flavor f with mass $m_f = \{m_{ud}, m_s, m_c, m_b\}$ and $\Gamma_C^\alpha = i\gamma_\alpha t^C$. For the spectra of quark-antiquark and di-gluon bound states we solve Bethe-Salpeter type equations in [6]. The master equation for the meson mass reads [5]:

$$1 = \alpha_s \cdot \lambda_{JJ}(M_J^2, m_1, m_2) = \alpha_s \frac{16\pi C_J}{9} \int \frac{d^4 k}{(2\pi)^4} \iint dx dy e^{-ik(x-y)} U_N(x) \sqrt{D(x)D(y)} \\ \times U_N(y) \text{Tr} \left[O_J \tilde{S}_{m_1}(\hat{k} + \xi_1 \hat{p}) O_J \tilde{S}_{m_2}(\hat{k} - \xi_2 \hat{p}) \right] |_{-p^2=M_J^2}, \quad (2)$$

where $C_J = \{1, 1, 1/2, -1/2\}$, $\xi_i = m_i/(m_1 + m_2)$, $O_J = \{I, i\gamma_5, i\gamma_\mu, \gamma_5 \gamma_\mu\}$ and the gluon ($\tilde{D}(k)$) and quark propagator ($\tilde{S}_{m_i}(\hat{p})$) are represented in Euclidean momentum space.

Note, the polarization kernel $\lambda_{JJ}(-p^2)$ has to be diagonalized using a complete system of orthonormal functions $\{U_N\}$, where $N = \{n, l, \mu, \dots\}$ is a set of quantum numbers. The solution of Eq. (2) is nothing else but the solution of the corresponding ladder Bethe-Salpeter equation.

Ultraviolet divergences in the model have been removed by renormalization of wave function and charge, but infrared (IR) singularities remain because of integration over momentum k in Eq. (2). To avoid the appearance of the singularities in the mass formula, we follow theoretical predictions in favor of an IR-finite behavior of the gluon propagator [7] and introduce IR cutoffs on the limits of scale integrations for the propagators as follows:

$$D(x) = \frac{1}{4\pi^2 x^2} \rightarrow \frac{1}{4\pi^2} \int_{\Lambda^2/2}^{\infty} ds e^{-sx^2}, \quad \tilde{S}_{m_f}(\hat{p}) \rightarrow (i\hat{p} + m_f) \int_0^{1/\Lambda^2} dt e^{-t(p^2 + m_f^2)}, \quad (3)$$

where Λ is the mass scale parameter characterizing the IR confinement domain. These propagators are entire analytic functions in the Euclidean space for $\Lambda > 0$. Note, another type of IR confinement applied to whole 'quark-antiquark' loop in [4] that is used in Sect. 3.

Effective strong coupling in the IR region

The meson mass M_J is defined by Eq. (2) at given α_s , quantum numbers N and constituent quark masses $\{m_1, m_2\}$. And vice versa, α_s can be estimated for given mass. The QCD

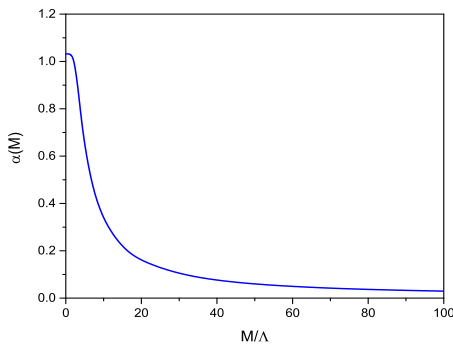


Figure 1. Effective strong coupling α_s in dependence on the relative mass scale M/Λ . The slope of $\alpha_s(M/\Lambda)$ changes for different $\Lambda > 0$, but the origin $\alpha_s(0) = 1.032$ remains fixed

coupling may feature an IR-finite behavior (e.g., in [8]). To study this, we consider M_J as

an appropriate energy-scale for α_s and choose a specific case $m_1 = m_2 \sim M/2$. Then, a new effective (mass-dependent) strong coupling $\alpha_s(M)$ in time-like domain reads:

$$\alpha_s(M) = -1/\lambda(M, M/2, M/2). \quad (4)$$

The dependence of the effective strong coupling $\alpha_s(M/\Lambda)$ on a relative mass scale M/Λ is shown in Fig. 1. Generally, the slope of $\alpha_s(M/\Lambda)$ changes for different $\Lambda > 0$, but the newly revealed origin $\alpha_s^0 = \alpha_s(0) = 1.032$ remains unchanged. This upper bound to the IR-fixed value $\alpha_s^0/\pi = 0.328$ is in a reasonable agreement with often quoted estimate in [9].

Lowest glueball state

The existence of glueballs, the bound states of gluons, is predicted by QCD because of the self-interaction of gluons. There are predictions expecting glueball-like states in the mass range $M_G \sim 1.5 \div 5.0$ GeV with spin $J = 0, 1, 2, 3$ [2]. Below we consider a two-gluon scalar bound state with $J^{PC} = 0^{++}$ and define the scalar glueball mass $M_{0^{++}}$ from the equation:

$$1 - \frac{8\alpha_s(M_{0^{++}})}{3\pi} \int dz e^{izp} \Pi_G(z) = 0, \quad p^2 = -M_{0^{++}}^2, \quad (5)$$

where $\Pi_G(z)$ is the self-energy (polarization) function of the scalar glueball.

Particularly, for $\Lambda = 236$ MeV and $\alpha(M_G)$ defined from Eq. (4) we obtain new estimates:

$$M_{0^{++}} = 1739 \text{ MeV}, \quad \alpha_s(M_{0^{++}}) = 0.451. \quad (6)$$

The new value of $M_{0^{++}}$ is in reasonable agreement with other predictions [2, 6, 10–12].

We also have obtained the scalar glueball 'radius' ($r_{0^{++}}$) that valued a often referred combination as follows: $r_{0^{++}} \cdot M_{0^{++}} = 4.41$ in reasonable agreement with data in [2].

Meson spectrum

The dependence of meson mass on α_s and other model parameters is defined by Eq. (2). The kernel function λ_N is real and finite, that allows us to evaluate a variational solution to M_J . For the fixed above parameter $\Lambda = 236$ MeV and the $\alpha_s(M)$ defined in Eq. (4) we derive meson mass formula Eq. (2) by fitting the conventional meson masses with adjustable constituent quark masses $\{m_{ud}, m_s, m_c, m_b\}$. We have fixed the final set of model parameters (in units of MeV) as follows:

$$\Lambda = 236, \quad m_{ud} = 227.6, \quad m_s = 420.1, \quad m_c = 1521.6, \quad m_b = 4757.2 \quad (7)$$

and represent in Tab. 1 our new estimates on the pseudoscalar (P) and vector (V) meson masses.

Table 1. Estimated masses of conventional mesons compared to the experimental data

$J^{PC} = 0^{-+}$	M_P (MeV)	Data [2]	$J^{PC} = 1^{--}$	M_V (MeV)	Data
D	1893.6	1869.62	ρ	774.3	775.26
D_s	2003.7	1968.50	K^*	892.9	891.66
η_c	3032.5	2983.70	D^*	2003.8	2010.29
B	5215.2	5259.26	D_s^*	2084.1	2112.3
B_s	5323.6	5366.77	J/Ψ	3077.6	3096.92
B_c	6297.0	6274.5	B^*	5261.5	5325.2
η_b	9512.5	9398.0	Υ	9526.4	9460.30

Note, our estimates represented in Tab. 1 are in reasonable agreement with the recent experimental data [2] with relative errors less than 1.8 per cent.

Leptonic decay constants

The leptonic decay constants f_J are important properties of mesons. In order to describe adequately the known 'sawtooth'-type unsmooth dependence of measured values of f_J on meson masses (see Tab. 2), we have to introduce additional parameters R_J characterizing the meson 'size' (in units of mass) into the meson ground-state functions as follows: $\tilde{U}_R(k) = \int_0^1 ds h(s) \exp[-sk^2/R_J^2]$, where $h(s)$ is a smooth function. Then, by keeping our model parameters fixed above and by varying on R_J to fit recent data on f_J we calculate optimal meson 'sizes' and the leptonic decay constants represented in Tab. 2.

Table 2. Estimated leptonic decay constants of mesons f_J (in MeV) compared to the experimental data

0^{-+}	R_f	f_P	Data	Ref.	1^{--}	R_P	f_V	Data	Ref.
D	0.93	207	206.7 ± 8.9	[13]	ρ	0.33	221	221 ± 1	[13]
D_s	1.08	257	257.5 ± 6.1	[13]	K^*	0.38	217	217 ± 7	[13]
η_c	1.83	238	238 ± 8	[14]	D^*	0.78	245	245 ± 20	[15]
B	1.73	193	192.8 ± 9.9	[16]	D_s^*	0.90	271	272 ± 26	[15]
B_s	2.18	239	238.8 ± 9.5	[16]	J/Ψ	2.40	416	415 ± 7	[13]
B_c	3.34	488	489 ± 5	[14]	B^*	3.34	196	196 ± 44	[15]
η_b	3.80	800	801 ± 9	[14]	Υ	2.80	715	715 ± 5	[13]

3 Dominant radiative decays of charmonium orbital excitations

Nowadays, the charmonium states are intensively searched in different experiments [17].

The CCQM [4] represents an appropriate theoretical framework to perform the analysis of the recent measurement of the dominant (one-photon) radiative decays $\chi_{cJ} \rightarrow J/\Psi + \gamma$ of the excited charmonium states χ_{cJ} , ($J = 0, 1, 2$) reported by the LHCb Collaboration [18].

The invariant matrix element for the decay $\chi_{cJ} \rightarrow \gamma + J/\Psi$ reads:

$$\mathcal{M}(\chi_{cJ}(p) \rightarrow J/\Psi(q_1) + \gamma(q_2)) = i(2\pi)^4 \delta^{(4)}(p - q_1 - q_2) \varepsilon_\chi^\Gamma \varepsilon_{J/\Psi}^\rho \varepsilon_\gamma^\sigma T_{\Gamma\rho\sigma}(q_1, q_2), \quad (8)$$

where $\{p, q_1, q_2\}$ and $\{\varepsilon_\chi^\Gamma, \varepsilon_\gamma^\rho, \varepsilon_{J/\Psi}^\sigma\}$ are the momenta and polarization vectors of $\{\chi_{cJ}, J/\Psi\}$ mesons and photon, correspondingly. In the leading order (LO), the matrix elements in Eq. (8) correspond to the Feynman diagrams of 'triangle' and 'bubble' types. Particularly, the LO amplitude given by the 'triangle' diagram reads:

$$T_{\Gamma\rho\sigma}(q_1, q_2) = g_\chi g_{J/\Psi} e_c e N_c \int \frac{d^4k}{(2\pi)^4 i} \tilde{\Phi}_\chi(-k^2) \tilde{\Phi}_{J/\Psi}(-k^2) \times \text{tr} \left[\gamma_\rho S(\hat{k} + \frac{1}{2}\hat{p}) \Gamma_\chi S(\hat{k} - \frac{1}{2}\hat{p}) \gamma_\sigma S(\hat{k} - \frac{1}{2}\hat{p} + \hat{q}_2) \right], \quad (9)$$

where $N_c = 3$, e_c and e are the electric charge of c-quark and electron; $S(\hat{k})$ is the c-quark propagator, $\Gamma_\chi = \{I, \gamma_\mu \gamma_5, i(\gamma_\mu k_\nu + \gamma_\nu k_\mu)\}$ stand for the scalar, axial-vector and tensor currents in $\chi = \{\chi_{c0}, \chi_{c1}, \chi_{c2}\}$ states.

The vertices $\tilde{\Phi}_\chi(-k^2)$ and $\tilde{\Phi}_{J/\Psi}(-k^2)$ are Gaussian functions and are determined by $\Lambda_{\chi cJ}$ and $\Lambda_{J/\Psi}$ - the corresponding 'size' parameters of χ_{cJ} and J/Ψ mesons.

The renormalized couplings g_χ and $g_{J/\Psi}$ for mesons $\chi = \{\chi_{c0}, \chi_{c1}, \chi_{c2}\}$ and J/Ψ are defined according the CCQM from the 'compositeness' condition by involving corresponding self-energy (mass) functions of mesons (see, for details [4]).

The 'bubble' diagrams take the similar structure but involving two S -propagators for the 'self-energy' quark-antiquark loop in the trace.

Spin=0

The invariant matrix element for the decay $\chi_{c0} \rightarrow \gamma + J/\Psi$ of scalar charmonium takes the most general form with two independent four momenta (see, e.g. [19]):

$$\mathcal{M}_{SVg} \sim \varepsilon_\rho(q_1) \cdot \varepsilon_\sigma(q_2) \cdot T_{\rho\sigma}, \quad T_{\rho\sigma} = d \cdot (q_2^\rho q_1^\sigma - g_{\rho\sigma}(q_1 \cdot q_2)), \quad (10)$$

where $T_{\rho\sigma}$ is the gauge invariant transition amplitude while form factor d is determined by resolving Eq. (9) for $\Gamma_J = I$.

The decay width for the transition reads:

$$\Gamma(\chi_{c0} \rightarrow \gamma + J/\Psi) = \alpha/24 \cdot M_{\chi_{c0}}^3 \left(1 - M_{J/\Psi}^2/M_{\chi_{c0}}^2\right)^3 \cdot g_{\chi_{c0} \rightarrow \gamma + J/\Psi}^2, \quad (11)$$

where $\alpha = e^2/4\pi$ and the χ_{c0} -meson decay coupling $g_{\chi_{c0} \rightarrow \gamma + J/\Psi}$ is calculated by solving Eq. (9).

Spin=1

For the axial-vector meson the invariant matrix element of transition $\chi_{c1} \rightarrow \gamma + J/\Psi$ reads:

$$\mathcal{M}_{AVg} \sim \varepsilon_\mu(p) \cdot \varepsilon_\rho(q_1) \cdot \varepsilon_\sigma(q_2) \cdot T_{\mu\rho\sigma}, \quad (12)$$

where the polarization vectors $\varepsilon_\mu, \varepsilon_\rho, \varepsilon_\sigma$ satisfy the constraints of transversality, completeness and orthonormality (see, e.g. [4]).

By taking into account the on-mass shell conditions one can write down five seemingly independent Lorentz structures of the gauge invariant transition amplitude as follows:

$$\begin{aligned} T_{\mu\rho\sigma}(q_1, q_2) &= \epsilon^{q_2\mu\sigma\rho}(q_1 \cdot q_2) W_1 + \epsilon^{q_1q_2\sigma\rho} q_1^\mu W_2 \\ &+ \epsilon^{q_1q_2\mu\rho} q_2^\sigma W_3 + \epsilon^{q_1q_2\mu\sigma} q_1^\rho W_4 + \epsilon^{q_1\mu\sigma\rho}(q_1 \cdot q_2) W_5 \end{aligned} \quad (13)$$

with five independent terms. Further, by revealing specific symmetry relations between four-dimensional tensors $\epsilon^{\mu\nu\rho\sigma}$ one can reduce the number of independent Lorentz structures and rewrite down the gauge invariant transition amplitude as follows [20]:

$$T_{\mu\rho\sigma} = \epsilon^{q_1q_2\mu\rho} q_2^\sigma \left(W_1 + W_3 - \frac{M_{J/\Psi}^2}{(q_1 \cdot q_2)} W_4 \right) + \epsilon^{q_1q_2\sigma\rho} q_1^\mu \left(W_1 + W_2 - \left(1 + \frac{M_{J/\Psi}^2}{(q_1 \cdot q_2)} \right) W_4 \right), \quad (14)$$

where form factors W_i ($i = 1, 2, 3, 4$) are determined by evaluating Eq. (9) for $\Gamma_{\chi_{c1}} = \gamma_\mu \gamma_5$.

The decay width of the one-photon radiative transition of axial-vector meson reads:

$$\Gamma(\chi_{c1} \rightarrow \gamma + J/\Psi) = 1/(12\pi M_{\chi_{c1}}^2) (|H_L|^2 + |H_T|^2) (M_{\chi_{c1}}^2 - M_{J/\Psi}^2)/2M_{\chi_{c1}}, \quad (15)$$

where the helicity amplitudes H_L and H_T are expressed in terms of the Lorentz amplitudes W_i and physical masses $M_{\chi_{c1}}$ and $M_{J/\Psi}$ [20].

Spin=2

The invariant matrix element for the tensor meson radiative decay $\chi_{c2} \rightarrow \gamma + J/\Psi$ reads:

$$\mathcal{M}_{TVg} \sim \varepsilon_{\mu\nu}(p) \cdot \varepsilon_\rho(q_1) \cdot \varepsilon_\sigma(q_2) \cdot T_{\mu\nu\rho\sigma}, \quad (16)$$

where the polarization vectors $\varepsilon_{\mu\nu}, \varepsilon_\rho, \varepsilon_\sigma$ satisfy the transversality, tracelessness, completeness and orthonormality conditions. The Lorentz conditions for vector meson and photon, and the gauge invariance of the transition amplitude result in two independent Lorentz structures of the gauge invariant transition amplitude as follows:

$$\begin{aligned} T_{\mu\nu\rho\sigma} &= A \cdot (g^{\mu\rho} [g^{\sigma\nu}(q_1 \cdot q_2) - q_1^\sigma q_2^\nu] + g^{\nu\rho} [g^{\sigma\mu}(q_1 \cdot q_2) - q_1^\sigma q_2^\mu]) \\ &+ B \cdot (g^{\sigma\rho} [q_1^\mu q_2^\nu + q_1^\nu q_2^\mu] - g^{\mu\sigma} q_1^\nu q_2^\rho - g^{\nu\sigma} q_1^\mu q_2^\rho), \end{aligned} \quad (17)$$

where two independent form factors A and B are determined by evaluating Eq. (9) for $\Gamma_{\chi_{c2}} = i(\gamma_{\mu}k_{\nu} + \gamma_{\nu}k_{\mu})$. The decay width of the one-photon radiative transition of tensor meson reads:

$$\Gamma(\chi_{c2} \rightarrow \gamma + J/\Psi) = \alpha/20 \cdot M_{\chi_{c2}}^3 \left(1 - M_{J/\Psi}^2/M_{\chi_{c2}}^2\right) \cdot g_{\chi_{c2} \rightarrow \gamma + J/\Psi}^2, \quad (18)$$

where the decay coupling $g_{\chi_{c2} \rightarrow \gamma + J/\Psi}$ of χ_{c2} meson is calculated by resolving Eq. (9) in the CCQM approach.

The obtained results of estimations for the dominant one-photon radiative decay widths $\Gamma(\chi_{cJ} \rightarrow J/\Psi + \gamma)$ of the charmonium orbital excitations for the CCQM model parameters $m_c = 1.68$ GeV (the constituent mass of c-quark) and $\lambda = 0.181$ GeV (the universal confinement scale) are represented in Tab. 3 in comparison with the recent experimental data [2].

Table 3. Estimated dominant one-photon radiative decay widths $\Gamma(\chi_{cJ} \rightarrow J/\Psi + \gamma)$ (in units of MeV) of the charmonium orbital excitations in comparison with the recent experimental data [2]

Meson	Mass	Γ_{tot}^{exp} (MeV)	$BR(\gamma + J/\Psi)$	Γ^{exp}	Γ^{theor}
$\chi_{c0} (0^{++})$	3414.71 ± 0.30	10.8 ± 0.6	$(1.40 \pm 0.05)\%$	0.151 ± 0.014	0.150
$\chi_{c1} (0^{++})$	3510.67 ± 0.05	0.84 ± 0.04	$(34.3 \pm 1.0)\%$	0.288 ± 0.022	0.289
$\chi_{c2} (0^{++})$	3556.17 ± 0.07	1.97 ± 0.09	$(19.0 \pm 0.5)\%$	0.374 ± 0.027	0.373

References

- [1] S. Bethke, Eur. Phys. J. C **64**, 689 (2009)
- [2] M. Tanabashi et al. (Particle Data Group), Phys. Rev. D **98**, 030001 (2018)
- [3] G.V. Efimov and G. Ganbold, Phys. Rev. D **65**, 054012 (2002). G. Ganbold, Phys. Part. Nuc., **43**, 79 (2012). Phys. Part. Nuc. **45**, 10 (2014)
- [4] T. Branz, A. Faessler, T. Gutsche, M. A. Ivanov, J. G. Körner and V. E. Lyubovitskij, Phys. Rev. D **81**, 034010 (2010). G. Ganbold, T. Gutsche, M. A. Ivanov and V. E. Lyubovitski, J. Phys. G: Nucl. Part. Phys. **42**, 075002 (2015). M.A. Ivanov, J.G. Körner and C.T. Tran, Phys. Rev. D **94**, 094028 (2016)
- [5] G. Ganbold, Phys. Rev. D **81**, 094008 (2010)
- [6] G. Ganbold, Phys. Rev. D **79**, 034034 (2009)
- [7] C. S. Fischer, R. Alkofer and H. Reinhardt, Phys. Rev. D **65**, 094008 (2002)
- [8] S. J. Brodsky and de G. F. Teramond, Phys. Lett. B **582**, 211 (2004)
- [9] M. Baldicchi et al., Phys. Rev. D **77**, 034013 (2008)
- [10] C. J. Morningstar and M. Peardon, Phys. Rev. D **60**, 034509 (1999)
- [11] Y. Chen et al., Phys. Rev. D **73**, 014516 (2006)
- [12] E. Gregory et al., J. High Energ. Phys. **10**, 170 (2012)
- [13] K. A. Olive et al. (Particle Data Group Collaboration), Chin. Phys. C **38**, 090001 (2014)
- [14] T.-W. Chiu et al. (TWQCD Collaboration), Phys. Lett. B **651**, 171 (2007)
- [15] D. Becirevic et al., Phys. Rev. D **60**, 074501 (1999)
- [16] J. Laiho, E. Lunghi and R. S. van de Water, Phys. Rev. D **81**, 034503 (2010)
- [17] R. Aaij et al. (LHCb Collaboration), Phys. Rev. D **92**, 112009 (2015). M. Ablikim et al. (BESIII Collaboration), Phys. Rev. Lett. **115**, 221805 (2015). A. Zupanc et al. (Belle Collaboration), Phys. Rev. Lett. **113**, 042002 (2014)
- [18] R. Aaij et al. (LHCb Collaboration), Eur. Phys. J. C **77**, 609 (2017)
- [19] D. Gamermann, E. Oset and B. S. Zou, Eur. Phys. J. A **41**, 85 (2009)
- [20] S. Dubnicka, A.Z. Dubnickova, M.A. Ivanov, J.G. Körner, P. Santorelli and G.G. Saidul-laeva, Phys. Rev. D **84**, 014006 (2011)